

Supporting Information

Mo-based crystal POMOFs with high electrochemical capacitor performance

Dongfeng Chai,^{a,b} Jianjiao Xin,^a Bonan Li,^a Haijun Pang,^{*a} Huiyuan Ma,^{*a} Kunqi Li,^a Boxin Xiao,^a Xinming Wang^a and Lichao Tan^a

Contents

Figure S1. The IR spectrum of btx ligand.....	Page 2
Figure S2. The ¹ H NMR of btx ligand.....	Page 2
Figure S3. The IR spectra of two compounds.....	Page 2
Figure S4. The XPS spectrum of 1	Page 3
Figure S5. Experimental and simulative PXRD patterns of two compounds.....	Page 3
Figure S6. The 78-membered macrocycle of Cu-MOF square lattices.....	Page 3
Figure S7. The distorted octahedron geometry of Cu(II) cation.....	Page 4
Figure S8. The plots of cathodic peak currents for 1 - and 2 -based electrodes vs. scan rates.	Page 4
Figure S9. The comparison of capacitance performance of compound 1 and two main parts.....	Page 5
Figure S9-1. The IR spectra of PMo ₁₂ and TBAT@PMo₁₂	Page 6
Figure S9-2. The IR spectra of btx ligand and Cu-MOF	Page 6
Figure S10. CV curves of two compounds at different scan rates.....	Page 6
Figure S11. The proposed equivalent circuit for the electrochemical capacitor...Page	7
Figure S12. FTIR spectra of compounds 1 and 2 immersed in H ₂ SO ₄	Page 7
Table S1. Selected bonds lengths (Å) and angles (°) for compound 1	Page 8
Table S2. Selected bonds lengths (Å) and angles (°) for compound 2	Page 9
Table S3. Summary of the typical MOF-based and POM-based supercapacitor electrodes at 3-electrode configuration.....	Page 10
Table S4. The calculated values of R _s and R _{ct}	Page 12

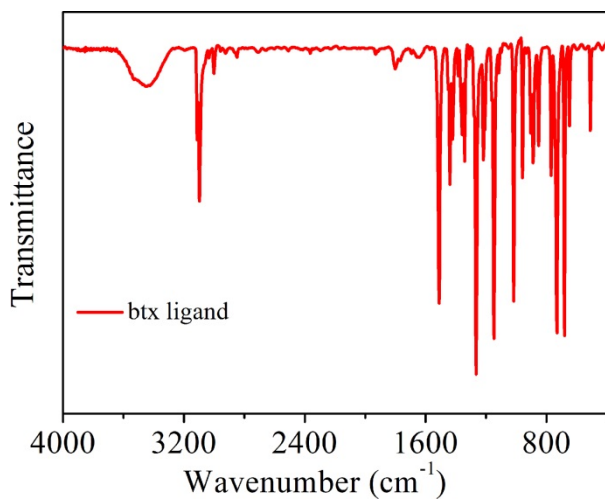


Figure S1. The IR spectrum of ligand of 1,4-bis(triazol-1-ylmethyl) benzene (btx).

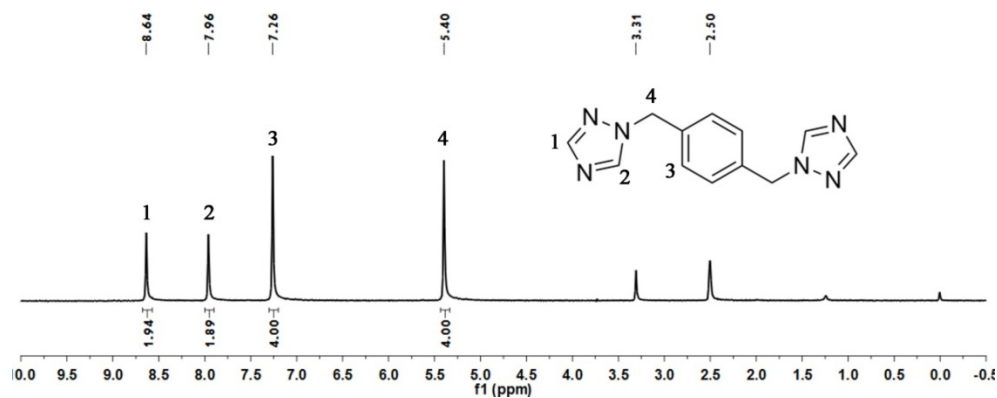


Figure S2. The ¹H NMR of ligand of 1,4-bis(triazol-1-ylmethyl) benzene (btx).

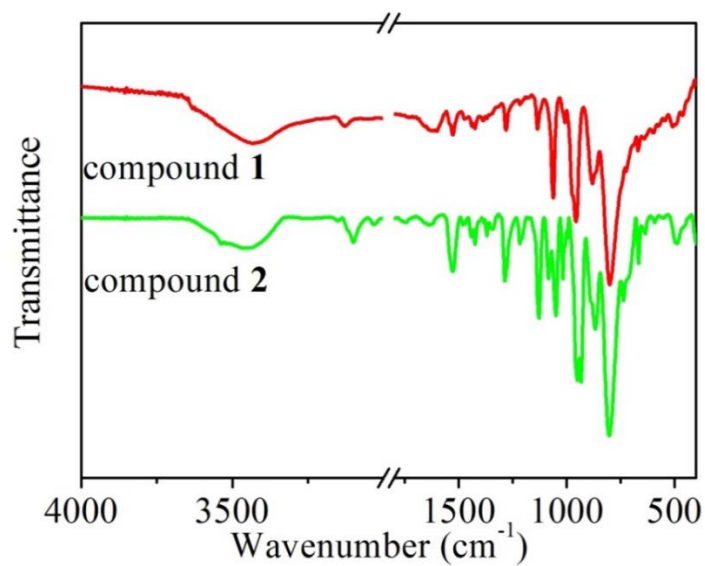


Figure S3. The IR spectra of compounds **1** (red line) and **2** (green line).

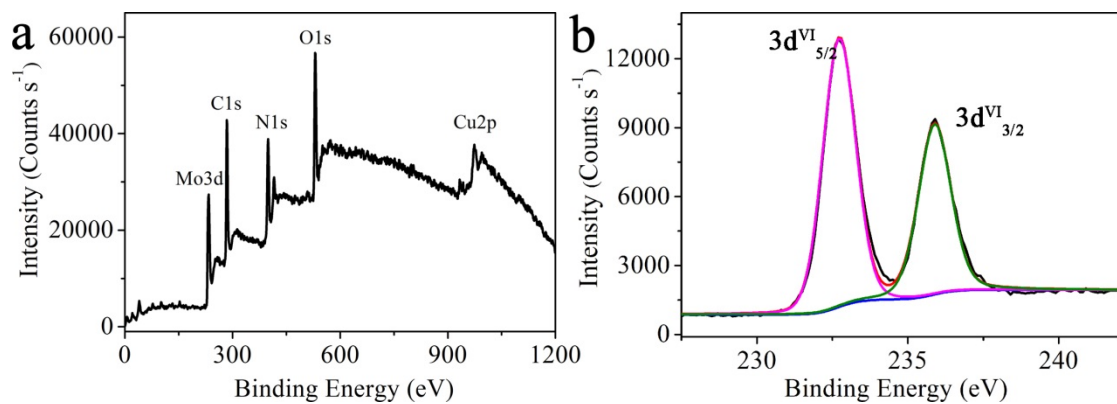


Figure S4. The XPS survey spectrum of **1** and high-resolution XPS spectrum of Mo (3d).

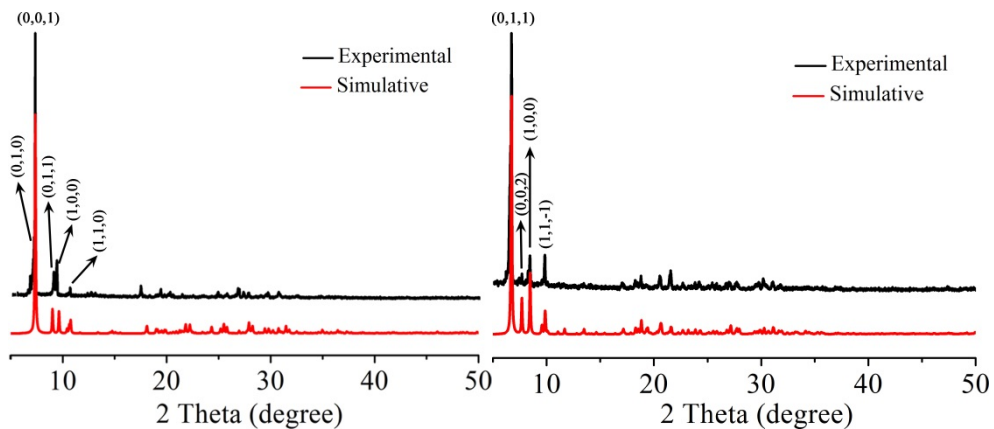


Figure S5. Experimental (black lines) and simulative (red lines) powder X-ray diffraction patterns of compounds **1** and **2**.

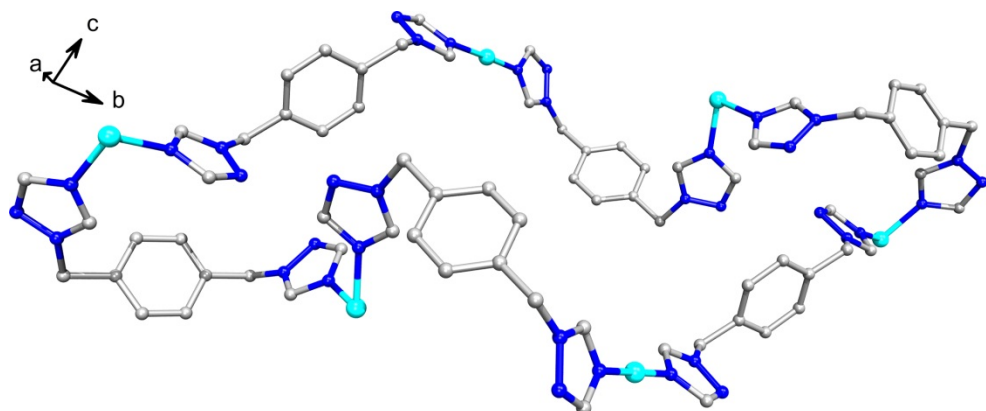


Figure S6. Six Cu(II) cations and six btx ligands are included in 78-membered macrocycle Cu-MOF square lattices.

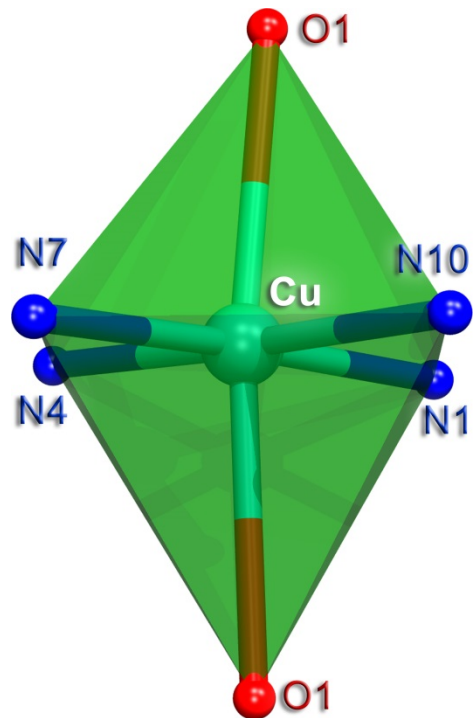


Figure S7. The distorted octahedron geometry of Cu(II) cation in compound **2**.

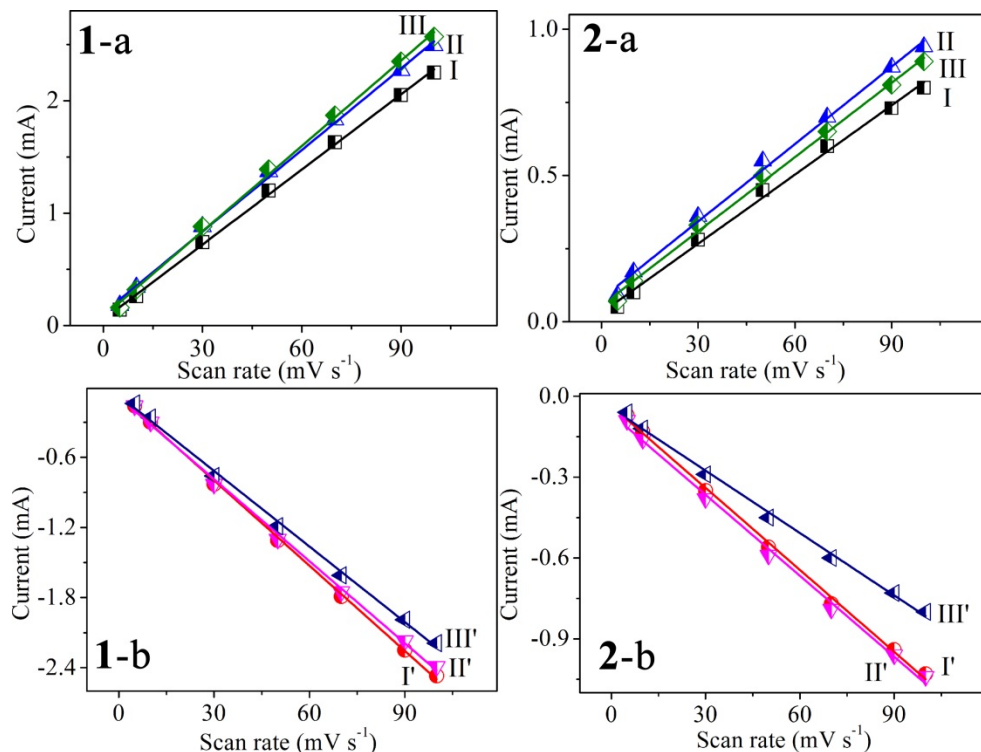


Figure S8. The plots of cathodic peak currents for **1**- and **2**-based electrodes vs. scan rates.

In order to demonstrate which section does contribute more for capacitance performance, the parent POM (**PMo@TBAB**) and the bare MOF particle (**Cu-MOF**) were prepared, and then **PMo@TBAB** and **Cu-MOF** were used as electrode materials to measure the capacitance performance, as shown in Figure S9.

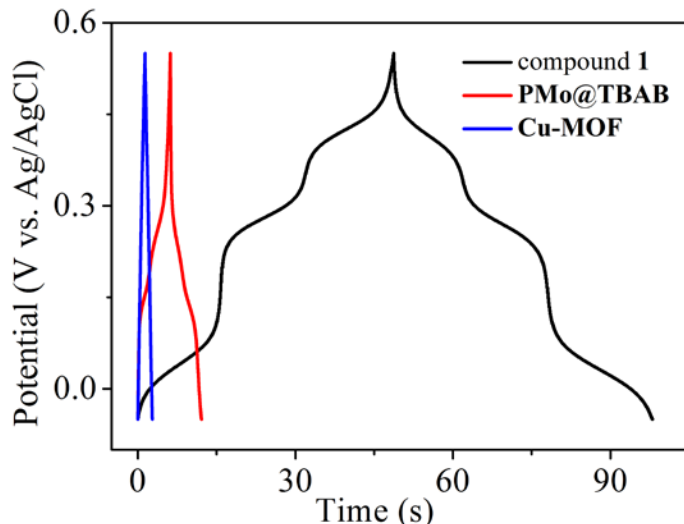


Figure S9. The comparison of capacitance performance of compound **1**, **PMo@TBAB** and **Cu-MOF**.

Synthesis of PMo@TBAB: Firstly, a solution of 0.1160 g (0.06 mmol) of PMo_{12} dissolving in 20 mL of distilled water was added to the solution of 5 mL of distilled water containing 0.0580 g (0.18 mmol) of tetrabutylammonium bromide (TBAB) under stirring, and a resulting suspension was filtrated, and the precipitate was collected, washed with distilled water three times, and dried in the oven at 80 °C for 5 h, then **PMo@TBAB** was obtained. Then **PMo@TBAB** was characterized by IR spectrum (Figure S9-1).

Synthesis of Cu-MOF: **Cu-MOF** was prepared by an identical synthesis method with compound **1** except that the POMs had not been added into the reaction system and the green color powder was collected, washed with distilled water three times, and dried in the oven at 80 °C for 5 h, then **Cu-MOF** can be obtained. Then **Cu-MOF** was characterized by IR spectrum (Figure S9-2).

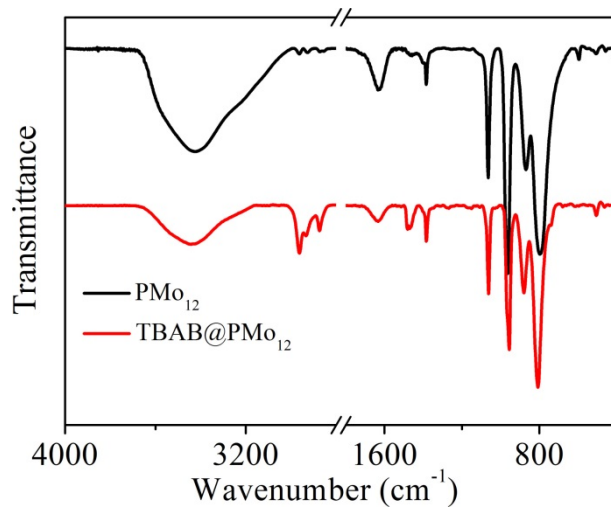


Figure S9-1. The IR spectra of **PMo₁₂** and **TBAB@PMo₁₂**.

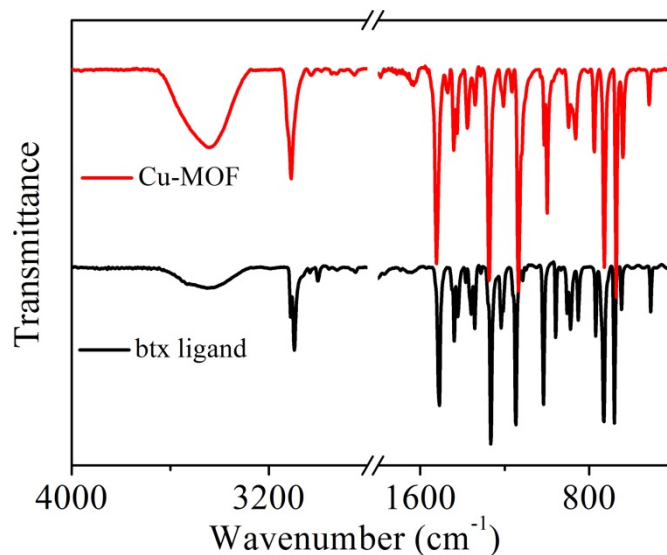


Figure S9-2. The IR spectra of btix ligand and **Cu-MOF**.

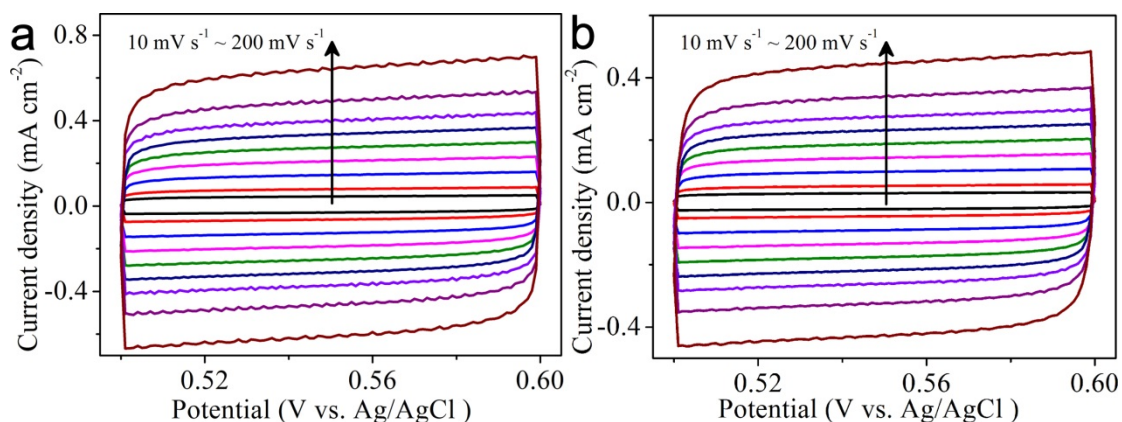


Figure S10. CV curves of **1** (a) and **2** (b) at different scan rates of 10, 20, 40, 60, 80, 100, 120, 150 and 200 mV s⁻¹.

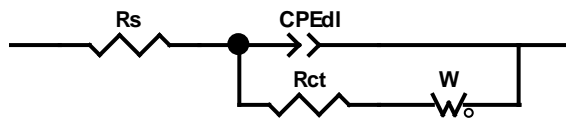


Figure S11. The proposed equivalent circuit for the electrochemical capacitor (R_s reflects the resistance of electrolyte and R_{ct} reflects the charge-transfer process).

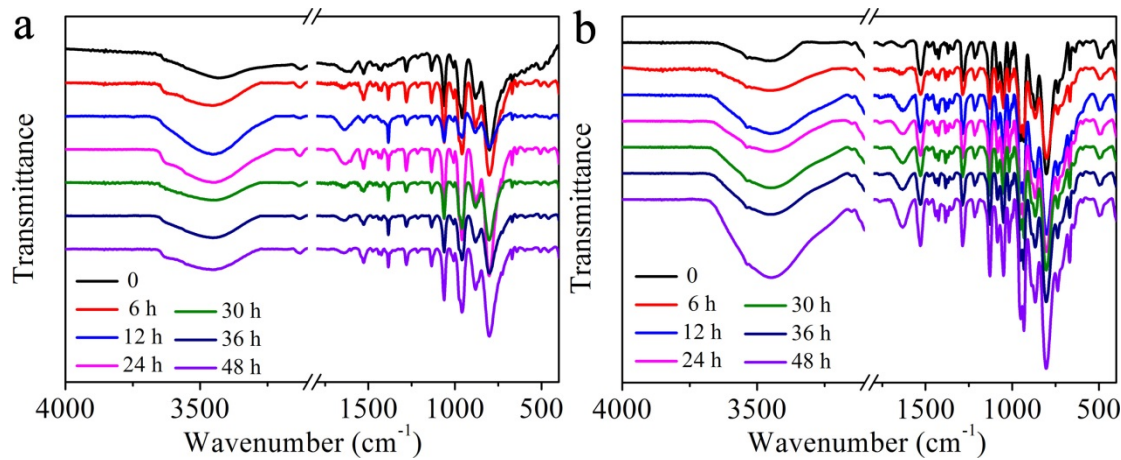


Figure S12. FTIR spectra of compounds **1** and **2** immersed in H_2SO_4 for 0, 6, 12, 24, 30, 36 and 48 h, respectively.

Table S1. Selected bond lengths (\AA) and angles ($^\circ$) for compound **1**.

Compound 1					
P-O(1A)	1.485(6)	Mo(1)-O(2B)	2.448(6)	N(3)-C(1)	1.314(7)
P-O(1A)#1	1.485(6)	Cu-N(1)	1.882(5)	N(3)-N(2)	1.351(7)
P-O(1B)#1	1.505(6)	Cu-N(1)#2	1.882(5)	N(3)-C(3)	1.467(7)
P-O(1B)	1.505(6)	Mo(3)-O(7)	1.653(4)	C(4)-C(6)	1.369(8)
P-O(2A)#1	1.541(6)	Mo(3)-O(9)	1.816(5)	C(4)-C(5)	1.379(8)
P-O(2A)	1.541(6)	Mo(3)-O(4)	1.826(4)	C(4)-C(3)	1.507(8)
P-O(2B)	1.578(6)	Mo(3)-O(8)	1.969(5)	C(5)-C(6)#3	1.389(9)
P-O(2B)#1	1.578(6)	Mo(3)-O(6)	2.005(5)	C(6)-C(5)#3	1.389(9)
Mo(1)-O(1)	1.647(4)	Mo(3)-O(2A)	2.424(6)	N(4)-C(9)	1.447(15)
Mo(1)-O(12)#1	1.828(5)	Mo(3)-O(1B)	2.491(6)	N(4)-C(11)	1.480(14)
Mo(1)-O(2)	1.832(5)	N(1)-C(1)	1.320(7)	N(4)-C(7)	1.827(17)
Mo(1)-O(3)	1.961(5)	N(1)-C(2)	1.356(8)	C(7)-C(8)	1.267(18)
Mo(1)-O(4)	1.969(4)	C(2)-N(2)	1.313(8)	C(11)-C(12)	1.436(16)
O(1A)-P-O(1A)#1	180.000(1)		O(1)-Mo(1)-O(12)#1	102.9(3)	
O(1A)-P-O(1B)#1	66.8(3)		O(1)-Mo(1)-O(2)	102.3(3)	
O(1A)#1-P-O(1B)#1	113.2(3)		O(12)#1-Mo(1)-O(2)	93.8(3)	
O(1A)-P-O(1B)	113.2(3)		O(1)-Mo(1)-O(3)	101.2(3)	
O(1A)#1-P-O(1B)	66.8(3)		O(12)#1-Mo(1)-O(3)	87.8(2)	
O(1B)#1-P-O(1B)	180.0(5)		O(2)-Mo(1)-O(3)	155.5(3)	
O(1A)-P-O(2A)#1	111.5(3)		O(1)-Mo(1)-O(4)	101.3(2)	
O(1A)#1-P-O(2A)#1	68.5(3)		N(4)-C(9)-C(10)	111.4(11)	
O(1B)#1-P-O(2A)#1	70.3(3)		N(1)-Cu-N(1)#2	180.000(1)	
O(1B)-P-O(2A)#1	109.7(3)		C(1)-N(1)-C(2)	103.3(5)	
O(1A)-P-O(2A)	68.5(3)		N(3)-C(3)-C(4)	111.9(5)	
O(1A)#1-P-O(2A)	111.5(3)		C(4)-C(5)-C(6)#3	120.5(6)	
O(1B)#1-P-O(2A)	109.7(3)		C(4)-C(6)-C(5)#3	120.1(6)	
Symmetry transformations used to generate equivalent atoms: #1 -x+1,-y+1,-z+1; #2 -x+1,-y+1,-z+2; #3 -x+2,-y,-z+2					

Table S2. Selected bond lengths (\AA) and angles ($^\circ$) for compound **2**.

Compound 2					
P-O(1B)	1.454(10)	Mo(1)-O(2B)	2.420(9)	C(17)-C(18)#5	1.371(14)
P-O(1B)#1	1.454(10)	Mo(1)-O(1A)	2.441(9)	C(17)-H(17)	0.9300
P-O(1A)#1	1.510(11)	Cu-N(4)	1.978(7)	C(18)-C(17)#5	1.371(14)
P-O(1A)	1.510(11)	Cu-N(10)	1.984(7)	C(18)-H(18)	0.9300
P-O(2B)#1	1.520(9)	Cu-N(1)	2.018(7)	C(22)-C(23)	1.361(13)
P-O(2B)	1.520(9)	Cu-N(7)	2.044(7)	C(23)-C(24)#6	1.361(15)
P-O(2A)#1	1.601(10)	Cu-O(1)	2.364(6)	C(23)-H(23)	0.9300
P-O(2A)	1.601(10)	C(3)-N(3)	1.467(12)	C(24)-C(23)#6	1.361(15)
Mo(1)-O(1)	1.672(6)	C(3)-C(10)#3	1.513(14)	C(24)-H(24)	0.9300
Mo(1)-O(4)	1.808(7)	C(3)-H(3A)	0.9700	N(2)-N(3)	1.326(11)
Mo(1)-O(5)	1.831(8)	C(3)-H(3B)	0.9700	N(5)-N(6)	1.316(11)
Mo(1)-O(3)	1.972(7)	C(10)-C(11)	1.377(13)	N(8)-N(9)	1.346(11)
Mo(1)-O(2)	1.980(8)	C(10)-C(3)#4	1.513(13)	N(11)-N(12)	1.344(10)
O(1)-Mo(1)-O(4)	102.1(4)		Mo(3)-O(7)-Mo(2)	135.3(4)	
O(1)-Mo(1)-O(5)	104.2(4)		Mo(3)-O(8)-Mo(3)#2	180.00(5)	
O(4)-Mo(1)-O(5)	94.9(4)		N(3)-C(3)-C(10)#3	112.2(8)	
O(1)-Mo(1)-O(3)	96.8(3)		N(3)-C(3)-H(3A)	109.2	
O(4)-Mo(1)-O(3)	87.5(3)		C(11)-C(10)-C(9)	117.1(10)	
O(5)-Mo(1)-O(3)	157.8(4)		C(11)-C(10)-C(3)#4	121.1(8)	
O(1)-Mo(1)-O(2)	98.8(4)		C(9)-C(10)-C(3)#4	121.7(9)	
O(4)-Mo(1)-O(2)	157.8(4)		C(18)#5-C(17)-H(17)	118.4	
O(5)-Mo(1)-O(2)	87.1(3)		C(17)#5-C(18)-C(16)	119.7(10)	
O(3)-Mo(1)-O(2)	82.6(3)		C(17)#5-C(18)-H(18)	120.2	
O(1)-Mo(1)-O(2B)	158.6(4)		C(24)#6-C(23)-C(22)	120.4(10)	
O(4)-Mo(1)-O(2B)	97.2(4)		C(24)#6-C(23)-H(23)	119.8	
O(5)-Mo(1)-O(2B)	64.6(4)		C(22)-C(24)-C(23)#6	121.6(10)	
Symmetry transformations used to generate equivalent atoms: #1 -x+1, -y+1, -z; #2 -x, -y+1, -z; #3 -x+1, y+1/2, -z+1/2; #4 -x+1, y-1/2, -z+1/2; #5 -x+1, -y, -z; #6 -x, -y, -z					

Table S3. Summary of the typical MOF-based and POM-based supercapacitor electrodes at 3-electrode configuration.

No.	Electrode	Current density	Specific capacitance	Ref.
1	HT-RGO-PMo ₁₂ (HT-RGO)	1 A g ⁻¹	276 (215) F g ⁻¹	Phys. Chem. Chem. Phys. 16(2014)20411
2	AC/PMo ₁₂ O ₄₀	2 A g ⁻¹	183 F g ⁻¹	Electrochim. Commun. 24(2012)35.
3	CNTs/PDDA/[P ₂ V-W ₁₇ O ₆₂] ⁸⁻	0.2 A g ⁻¹	82 Fg ⁻¹	J. Solid State Electr. 17(2013)1631
4	HPW/RGO	2 A g ⁻¹	153.8 F g ⁻¹	Compos. Part B-Eng. 121(2017)75
5	PPy-PMo ₁₂ /rGO	2 Ag ⁻¹	252 F g ⁻¹	Chem. Commun. 51(2015)12377
6	AC@PMo ₁₂ O ₄₀	1 mV s ⁻¹	223 F g ⁻¹	J. Power Sources 326(2016)569
7	MWCNT-PMo ₁₂	25 mV s ⁻¹	106.9 F cm ⁻³	Electrochim. Commun. 43(2014)60
8	Na ₆ V ₁₀ O ₂₈	2 A g ⁻¹	143 Fg ⁻¹	ChemPhysChem 15(2014)2162
9	PEDOT.[PV ₂ Mo ₁₀ -O ₄₀]; PEDOT.[PMo ₁₂ O ₄₀]	100 mV s ⁻¹	70; 140 F g ⁻¹	Electrochim. Acta 49(2004)861
10	Co ₈ -MOF-5	25 mV s ⁻¹	0.49 F g ⁻¹	Mater. Lett. 68(2012)126
11	Cu-CATNWAs	0.5 A g ⁻¹	202 F g ⁻¹	Adv. Funct. Mater. 2017, 1702067

12	ZIF-67	hierarchical flower-like structure	1 A g^{-1}	188.7 F g^{-1}	RSC	Adv.
13	UiO-66		5 mV s^{-1}	1144 F g^{-1}	RSC	Adv.
14	ZIF-67		0.5 A g^{-1}	168.3 F g^{-1}	Nano-Micro Lett.	
15	Layered Co-MOF nano sheets	structural	1 A g^{-1}	2564 F g^{-1}	Chem-A Eur. J.	
16	ZIF-67-CC		10 mV s^{-1}	1.47 mF cm^{-2}	J. Am. Chem. Soc	
17	V ^{IV} (O)(bdc)		0.5 A g^{-1}	572.1 F g^{-1}	Small	2018, 1801815
18	N-NFC		1 A g^{-1}	387.3 F g^{-1}	Nanoscale	
19	Cu@BTC-120		1.5 A g^{-1}	228 F g^{-1}	Appl. Surf. Sci.	
20	ZIF-8; ZIF-8@ZIF-67	ZIF-67;	2 A g^{-1}	$239; 119; 270 \text{ F g}^{-1}$	J. Am. Chem. Soc.	
						460(2018)33
						137(2015)1572

21	MOF-5	0.05 A g^{-1}	90 F g^{-1}	ACS Mater.	Appl. Interfaces
22	$[\text{Cu}_2(\text{C}_{12}\text{H}_{12}\text{N}_6)_4(\text{PMo}_{12}\text{O}_{40})_5 \text{A g}^{-1}]$		146.7 F g^{-1}	This work	7(2015)3655
23	$[\text{Cu}^{\text{I}}\text{H}_2(\text{C}_{12}\text{H}_{12}\text{N}_6)(\text{P}-\text{Mo}_{12}\text{O}_{40})_5 \cdot [(\text{C}_6\text{H}_{15}\text{N})_{12}(\text{H}_2\text{O})_2]$	5 A g^{-1}	239.2 F g^{-1}	This work	

Table S4. The calculated values of R_s and R_{ct} through the proposed equivalent circuit.

Compounds	$R_s(\Omega)$	$R_{ct}(\Omega)$
1	4.93	3.33
2	5.08	6.26